Preparation of Titanium Dioxide/Polyacrylate Nanocomposites by Sol–Gel Process in Reverse Micelles and *in situ* Photopolymerization

Tao Wan,[1,2] Yue-Chuan Wang,[1] Fei Feng[1]

[1]*College of Polymer Science and Engineering, State Key Laboratory of Polymer Materials Engineering, Sichuan University, Chengdu, People's Republic of China 610065*
[2]*College of Materials and Chemistry and Chemical Engineering, Chengdu University of Technology, Chengdu, People's Republic of China 610059*

Received 3 August 2005; accepted 26 December 2005
DOI 10.1002/app.24166
Published online in Wiley InterScience (www.interscience.wiley.com).

ABSTRACT: UV-curable, transparent acrylic resin/titania organic–inorganic hybrid films were prepared by controlled hydrolysis of titanium tetrabutoxide in Span-85/Tween 80 reverse micelles and the subsequent *in situ* photopolymerization of the acrylic monomers. UV–vis spectra and atomic force microscopy (AFM) indicated the presence of a nanoscale hybrid composition. The onset of absorption (λ_{onset}) of titania in the hybrids appeared between 363.4 and 383.5 nm, which exhibited blue shifts relative to that of bulk anatase ($\lambda_{onset} = 385$ nm). The titania content increased rapidly at higher temperature and higher TTB content, whereas it increased slowly with longer post-thermal treatment times. The refractive index and UV shielding properties of the organic polymer were obviously improved with increasing titania content. AFM images showed the inorganic domains (mean size 25.3–28.8 nm) were uniformly dispersed in the polymeric networks. The roughness parameters of the hybrid material were: toughness, 1.5–2.3 nm; root mean square roughness, 4.5–4.6 nm; and peak and valley distance, 9.7–19.4 nm. © 2006 Wiley Periodicals, Inc. J Appl Polym Sci 102: 5105–5112, 2006

Key words: micelles; nanocomposites; atomic force microscopy (AFM); irradiation

INTRODUCTION

As novel functional materials, hybrid organic–inorganic nanocomposites offer the opportunity to combine the desirable properties of organic polymers (toughness, elasticity) with those of inorganic solids (hardness, chemical resistance). Because these materials have been widely applied in many areas such as optics, electronics, ionics, mechanics, protective coatings, catalysis, sensors, and biology,[1–5] they have received much attention in the fields of material science.

The driving forces behind the intense activity in this area are the new and different properties of the nanocomposites that traditional macroscale composites and conventional materials do not have. For example, unlike traditional composite materials, which have macroscale domain size on a millimeter or even micrometer scale, most organic/inorganic hybrid materials are nanoscopic, with a physical constraint of several nanometers, typically 1–100 nm. Therefore, they often remain optically transparent materials although microphase separation may exist.

Correspondence to: Y. C. Wang (gycwang@163.net; wangyc@scu.edu.cn).

Journal of Applied Polymer Science, Vol. 102, 5105–5112 (2006)
© 2006 Wiley Periodicals, Inc.

Until now, there have been very few studies of the preparation of polymer/titania hybrid materials by the sol–gel method, although titania has good chemical stability and a high refractive index and dielectric constant.[6,7] Wang et al.[8] successfully prepared high-refractive-index organic–inorganic hybrid materials by using titanium tetraisopropoxide as the inorganic precursor to react with triethoxysilane-capped poly (arylene ether ketone) and poly(arylene ether sulfone). Lee and Chen[9] synthesized high-refractive-index PMMA–titania hybrid thin films that could potentially be used as optical thin films.

However, there have been no reports of the preparation of titania/polyacrylate nanocomposites formed by sol–gel processing in reverse micelles with subsequent *in situ* photopolymerization. The present study was the first to investigate the formation of transparent titania/polyacrylate nanocomposites via hydrolysis of titanium tetrabutoxide (TTB) in Span-85/Tween 80 reverse micelles and entrapment of nanosized titania particles by subsequent photopolymerization. The structure and optical properties of the hybrid films were investigated by atomic force microscopy (AFM) and ultraviolet-visible (UV–vis) spectroscopy, respectively. Transparent hybrid films with a tunable refractive index of 1.46–1.52 and small shrinkage and roughness potentially could be used as holographic recording materials.

EXPERIMENTAL

Materials

Chemical-grade butyl acrylate was Beijing Dongfong Chemical Factory (China) washed with 30 wt % NaOH solution three times. Analytic-grade acrylic acid was Beijing Dongfong Chemical Factory (China) used without further purification. Sorbite anhydride monostearic acid ester (Span-85) and commercial-grade Tween 80 [poly(oxyethylene sorbitan monooleate)], purchased from the Beijing Chemical Co. (China); titanium tetrabutoxide purchased from Yangzhov Lida Resin Co. (China); Darocur1173 (2-hydroxy-2-methylpropiophenone) provided by the Ciba Company (Summit, NJ); and chemical-grade trimethylolpropyltriacrylate purchased from Jiangsu Tianpeng Tongren Fine Chemical Co. (China) were used without further treatment.

Methods

Preparation of titania reverse micelles

Titania reversed micelles were synthesized with titanium tetrabutoxide (TTB) as a precursor alkoxide, Span-85 and Tween 80 as surfactants, butyl acrylate (BA) as the reactive solvent, acrylic acid (AA) as carboxylic acid ligand, trimethylolpropyltriacrylate (TMPTA) as crosslinker and bidistilled water for hydrolysis. First, 10 wt % Span-85 and Tween 80 were mixed in 20-mL mixtures of butyl acrylate and TMPTA, and then about 1 mL of water was added dropwise to form transparent reverse micelles. Finally, mixtures of acrylic acid and TTB were added carefully to the reverse micelles while the solution was stirred mildly. After hydrolysis of titanium butoxide at room temperature for at least 30 min, stable and clear titania reversed micelles were successfully obtained and used for the preparation of the hybrid films. The mass ratio of BA : TMPTA : surfactant : H_2O : TTB : AA was 100 : 20 : 10 : 5 : 30 : 15.

Preparation of titania–acrylic polymer hybrid films

The curing of the hybrid films was induced using UV irradiation. For that purpose, a photoinitiator, 2-hydroxy-2-methylpropiophenone (5 wt %, based on the total monomer weight), was added to the formulations. Hybrid organic–inorganic films were deposited via casting on precleaned soda-lime glass substrates. Photopolymerization was achieved by irradiating the samples with a 50 mW/cm^2 high-pressure mercury lamp. After about 6 min of irradiation, transparent hybrid films were obtained.

Characterizations

UV–visible absorption spectra were recorded on a Thermo Spectronic Genesys TM 10 series spectrophotometer with a quartz cuvette whose optical path length was 1 cm. The refractive indices of the hybrid materials were measured by an Abbe refractometer at 20°C. Film roughness and surface morphologies were examined by AFM measurements using a Digital Instruments NanoScope IIIa instrument in tapping mode with a silica probe (NSC 11) and a frequency of 65 KHz. Scan dimension and roughness analysis were performed on images 2 × 2 μm^2 in size. The roughness parameters, such as mean roughness and root mean square roughness, were obtained with AEM data software.

RESULTS AND DISCUSSION

Preparation of titania–acrylic polymer hybrid films

The sol–gel process is a powerful method for designing new materials based on the hydrolysis and condensation reactions of molecular precursors such as metal alkoxides. However, for titania-based materials the precursor alkoxides are very reactive, and direct hydrolysis usually leads to precipitates. For these systems, direct precipitation can be avoided by the addition of hydroxylated complexing ligands to the titanium precursor[10,11] or by confinement of water in reverse micelles.[12–14] In the micellar solution, hydrolysis may occur inside the micelle by penetration of the Ti precursor through the surfactant layer or, in the hydrocarbon phase, by reaction with water attached to the polar head of a surfactant molecule released from the micelle. Condensation reactions lead to formation of Ti—O—Ti bridges and particle growth. These particles are partially hydroxylated, and condensation reactions between them produce precipitates or generate a network enclosing the liquid phase. Both processes involve the rearrangement of surfactant molecules that either may be adsorbed into the partially hydroxylated skeleton or may form micelles in the solution phase. Therefore, the hydrolysis and condensation reactions were controlled by confinement of titania nanoparticles inside the micelles.

Titanium alkoxides are, in fact, known to readily react with carboxylic acids such as MAA[15–17] in mild conditions by competitive pathways: substitution, nonhydrolytic condensation and/or elimination of an ester that generates Ti—O—Ti bonds, or by hydrolysis–condensation after slow esterification.

In the present study reactive monomer butyl acrylate was used as the continuous oil phase and acrylic acid (AA) as the carboxylic acid ligand to further control the hydrolysis reaction and construct the chemical linkages between the organic and inorganic phases.

After the formation of stable and transparent titania reverse micelles, other components such as a photoinitiator were added, the mixtures were exposed to a high-pressure mercury lamp to irradiate for 6 min,

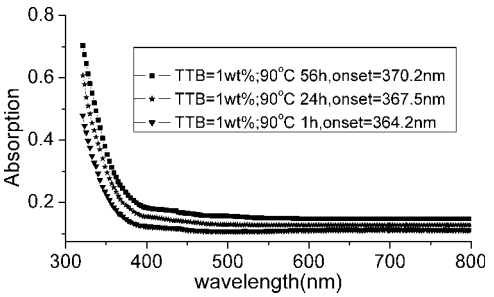

Figure 1 UV–vis absorption of hybrid film as a function of heat treatment time.

and finally the titania–acrylic polymer hybrid films were formed.

Optical properties

UV–vis spectroscopy was used to characterize the bulk structure of the crystalline and amorphous titanium dioxide. From the linear extrapolation of the steep part of the UV absorption toward the baseline, the energy of the lower excited state was determined. The onset of absorption (λ_{onset}) and the corresponding band-gap energy (Eg) of the bulk TiO_2 were determined to be 385 nm and 3.2 eV, respectively, for anatase,[18] and 415 nm and 3.0 eV, respectively, for rutile.[19]

In this experiment, a UV–vis spectrum of the reverse micelles using monomer as the continuous oil phase without TTB was used as reference, and we subtracted its value from the UV–vis spectra of the hybrid films. The UV–vis spectra obtained, as shown in Figures 1–3, were mainly a result of the scattering and absorbance of the nanosized titanium dioxide within the polymer matrix.

It is clear that as the particle size decreased the band-gap energy increased. Size quantization caused the absorption edge to be shifted to a higher energy. From the shift in the band gap (ΔEg), the particle size could be approximated using eq. (1):[20]

$$\Delta Eg = h^2\pi^2/2\mu R^2 - 1.786e^2/\varepsilon R(0.248E_{RY}) \qquad (1)$$

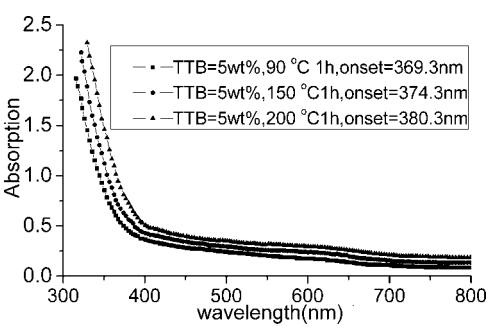

Figure 2 UV–vis absorption of hybrid film as a function of temperature of heat treatment.

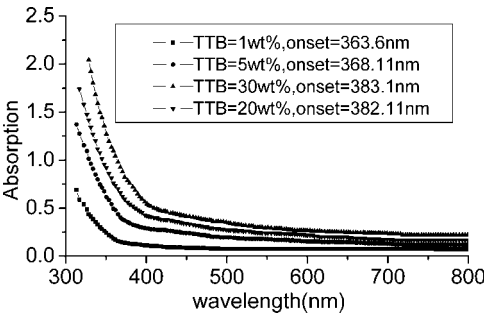

Figure 3 UV–vis absorption of hybrid film as a function of TTB concentration.

where R is the radius of the particle; h is Planck's constant; E_{RY}, is the effective Rydberg energy, μ is the reduced mass of the exciton, that is, the reduced effective mass of the electron and the hole in the semiconductor; e is the electronic charge (1.6×10^{-19} C); and ε is the dielectric constant of the semiconductor. The first term, proportional to R^{-2}, is the shift to a higher energy gap because of quantum localization, whereas the second term, proportional to R^{-1}, is the shift to a lower energy gap because of the electrostatic interaction between the electron and the hole. Using $\varepsilon = 184$ and $\mu = 1.63$ me (me $= 9.1 \times 10^{-28}$ g), as reported in the literature,[19] we were able to roughly estimate the particle size.

Figures 1–3 show the UV absorbance spectra of TiO_2/polyacrylate hybrid films prepared by the sol–gel process in reverse micelles with subsequent *in situ* photopolymerization. Figures 1–3 show that in general there was relatively low absorption of the hybrid films, in the range of 400–800 nm, indicating their excellent optical transparency in the visible region. According to the Rayleigh equation,[21] a smaller size of the aggregated titania resulted in less loss of optical scattering and increasing transparence of the hybrid films. Thus, the relative low absorbance in the visible region proved again that nanosized titania–acrylic polymer hybrid materials could be prepared using sol–gel approaches in reverse micelles with subsequent photopolymerization. Furthermore, strong absorbance, in the range of 300–400 nm, was observed for the hybrid films, which should be assigned to the electronic transitions of the Ti—O—Ti chains and the charge–transfer effect of the Ti—O—Ti segment.[22,23]

Above all, as shown in Figures 1–3, the onset of absorption (λ_{onset}) of TiO_2 particles of hybrid films of different compositions appeared between 363.4 and 383.5 nm, which exhibited blue shifts relative to the onset of bulk anatase ($\lambda_{onset} = 385$ nm).

After the sol–gel process followed by photopolymerization, the hybrid films were postheated in order to further enhance the polycondensation between TiOH and to remove the residual volatile molecules in the hybrids, and the corresponding UV–vis spectra are shown in Figure 1.

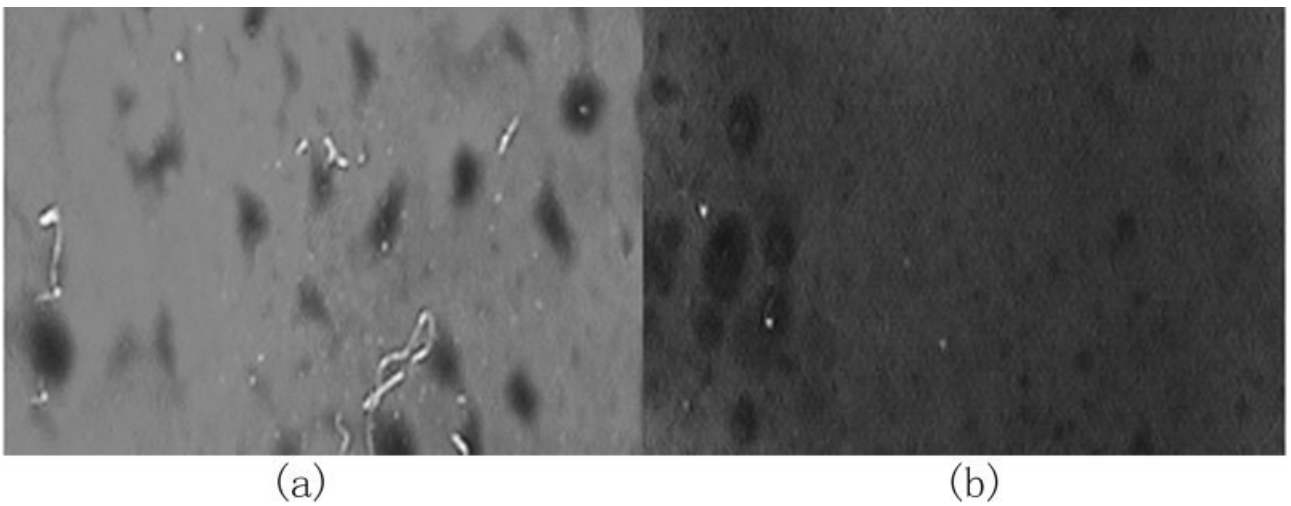

Figure 4 Pictures of (a) hybrid film with 30 wt % TTB and (b) pure acrylic polymer film after 60 min of UV irradiation by 1000W mercury lamp.

According to eq. (1), when the size of titania was small enough, the band-gap value increased, leading to the blue shift of the absorption edge. However, the absorption edge shifted to the low-energy side with increasing post-thermal time, as shown in Figure 1. This might be attributed to the increase in the size of the titania particles.

To further study the effect of post-thermal treatment on the UV–vis absorbance spectra of the hybrid films, three temperatures, 90°C, 150°C, and 200°C, were selected, and their UV–vis absorbance spectra are shown in Figure 2. The onset of absorption sharply increased from 369.3 to 380.3 nm with an increase in temperature from 90°C to 200°C, indicating remarkably aggregated titania during post-thermal treatment at higher temperatures.

It can be seen that post-thermal treatment at 90°C for 1–56 h caused the λ_{onset} to slightly increase from 364.2 to 370.2 nm. However, with post-thermal treatment at 200°C for only 1 h, the λ_{onset} increased from 369.3 to 380.3 nm, indicating post-thermal treatment temperature had a much more significant effect on λ_{onset} than did post-thermal treatment time.

In addition to post-thermal treatment, TTB concentration also significantly influenced the onset of absorption, as shown in Figure 3. Onset of absorption as well as Ti—O—Ti content dramatically increased with an increase in TTB concentration, for example. The λ_{onset} increased from 363.6 to 383.5 nm with an increase in TTB concentration from 1 to 30 wt %, which might be attributed to the increased size of titania.

The transmittance spectra of the hybrid films, even with 30 wt % TTB content, exhibited good optical transparence in the visible range (400–700 nm). But transmittance in the UV region decreased with increasing titania content in the hybrid films, suggesting that titania/acrylic polymer organic–inorganic hybrid materials could improve the UV-shielding property of the polymer without significantly decreasing the transparence.

The photostability of the hybrid film with 30 wt % TTB was compared with that of the pure acrylic polymer film after 60 min of UV irradiation by a 1000W mercury lamp, as shown in Figure 4. The hybrid film was red brown, whereas the pure acrylic polymer film was dark brown, indicating enhanced

TABLE I
TiO_2 Particle Sizes Obtained from UV–vis Spectra Shown in Figures 1–3

	Post–thermal treatment time (h) at 90°C			
	1	24	56	
Particle size (nm)	7.0	7.6	8.3	
	Post-thermal treatment temperature (°C)			
	90	150	200	
Particle size (nm)	8.1	9.9	14.7	
	TTB content (wt %)			
	1	5	20	30
Particle size (nm)	6.8	7.7	18.7	21.0

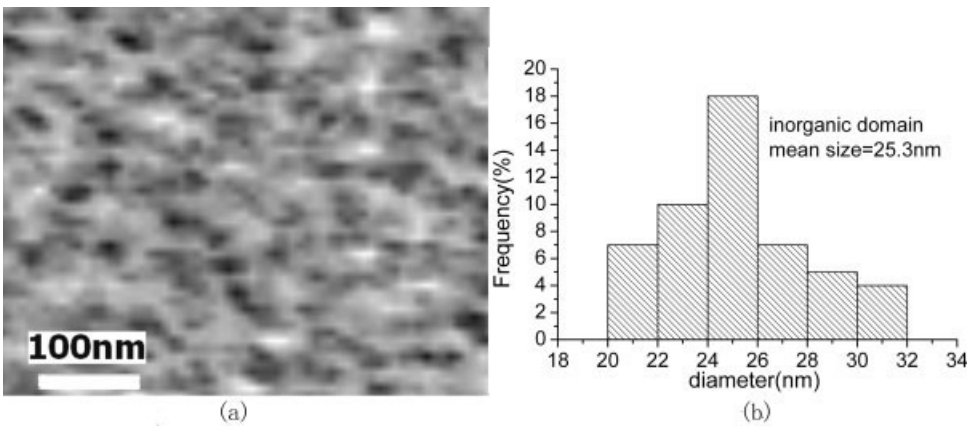

Figure 5 (a) AFM phase diagram and (b) inorganic domain size histogram of titania–acrylic polymer hybrid film without post-thermal treatment (TTB = 30 wt %, photocuring for 6 min).

photostability of the hybrid film. The TiO_2 in the hybrid films was amorphous (as indicated by XRD, not shown here) and could absorb and scatter the UV radiation. Therefore, amorphous TiO_2 had low photocatalysis and high photostabilization, and the hybrid films might achieve long-term UV protection and could be used as UV shielding materials.

Table I summarizes the data on titania particle radius estimated by eq. (1) with different parameters such as post-thermal treatment and TTB concentration. It can be seen that the titania particles synthesized in reverse micelles had calculated radii between 6.8 and 21.0 nm, and the particle size increased rapidly at higher post–thermal treatment temperatures and higher TTB concentrations and slowly at higher post–thermal treatment times.

AFM study

AFM can provide valuable information on nanoclusters and can serve as an ideal tool to characterize cluster-covered surfaces because a wide range of materials can be chosen as substrates for cluster deposition.

The bright and dark regions of the AFM phase images, as shown in Figures 5 and 6, corresponded to the inorganic and organic domains, respectively.

The AFM phase images show that the phase morphology of the hybrid films was closely correlated with the post-thermal treatment. The AFM micrographs of the hybrid films with and without post-thermal treatment show the presence of inorganic domains with mean sizes of 38.3 and 25.3 nm, respectively. This demonstrates that the inorganic domain size was related to post-thermal treatment.

Above all, the AFM phase images showed the presence of inorganic domains, whose mean size was 25.3–28.8 nm, uniformly dispersed in the polymeric network. Therefore, the new method used to prepare titania–acrylic polymer hybrid films by sol–gel processes in reverse micelles followed by rapid photopolymerization was effective.

In addition, the effects of post-thermal treatment on titania particle size could be further studied by

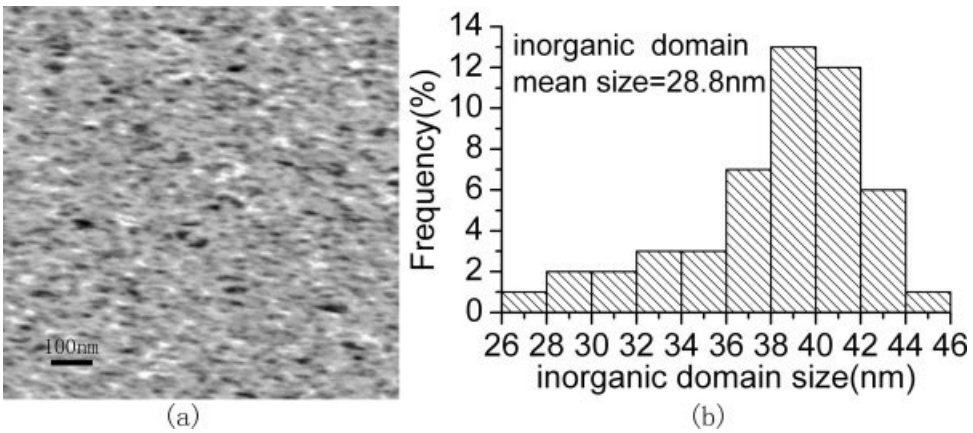

Figure 6 (a) AFM phase diagram and (b) inorganic domain size histogram of the titania–acrylic polymer hybrid film with post-thermal treatment (TTB = 30 wt %, photocuring for 6 min, post-thermal treatment: 90°C fpr 80 h).

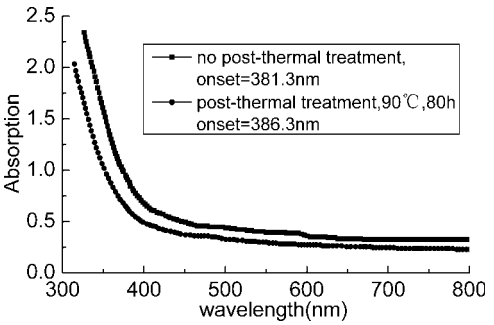

Figure 7 Effects of post-thermal treatment on UV–vis spectra of hybrid films at a mass fraction of 30% TTB.

UV–vis spectra. As shown in Figure 7, the λ_{onset} of the hybrid films increased from 383.1 to 386.3 nm after post-thermal treatment. This further demonstrated the increase of titania size during post-thermal treatment. In addition, the hybrid films exhibited excellent optical transparency in the visible region, an indication of nanoscale hybrid compositions. These results were consistent with those of the AFM images.

Roughness study by AFM

The darkest and brightest regions in the AFM images reported in this article corresponded to those regions with the largest height gradients. The brightness of a region corresponded directly to its height. For quantitative height information from each image, a line profile is given that shows the height of significant or typical features and the depth of pores.

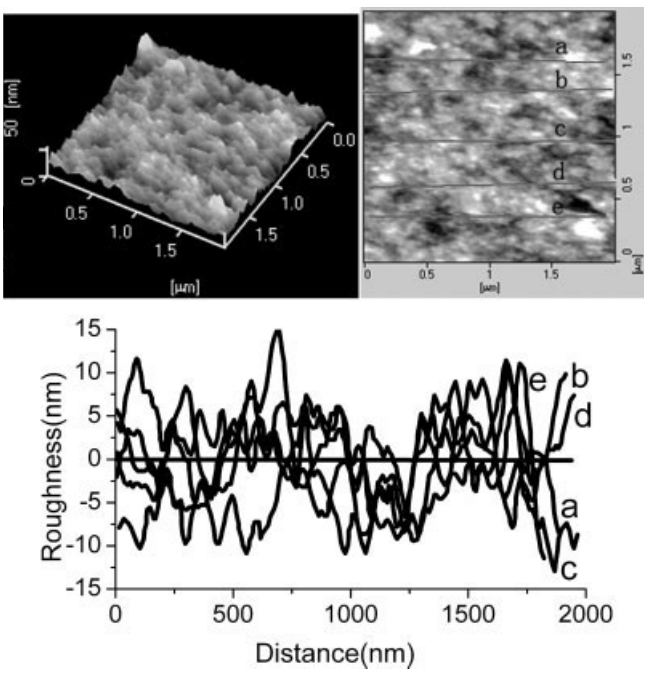

Figure 8 AFM topography and accompanying line profiles of the surfaces of hybrid films without post-thermal treatment (TTB = 30 wt %, photocuring for 6 min).

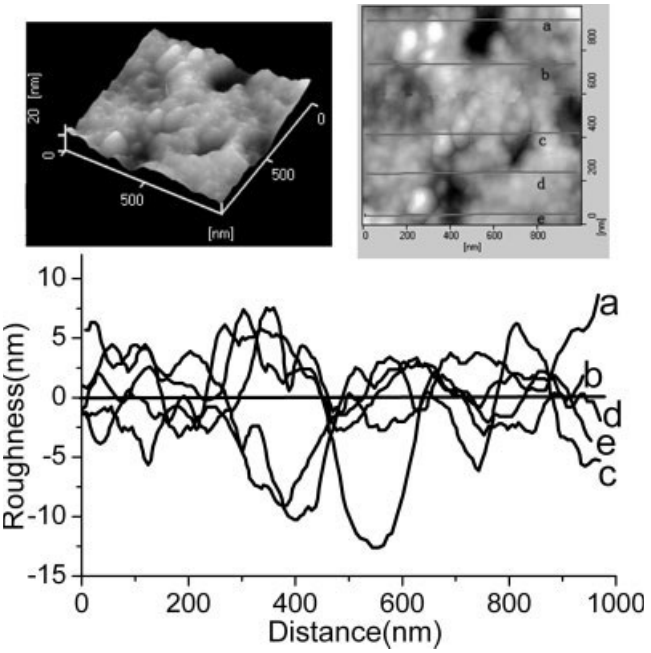

Figure 9 AFM topography and accompanying line profiles of TiO_2/polyacrylate film with post–heat treatment (TTB = 30 wt %, photocuring for 6 min, post–heat treatment: 90°C for 80 h).

Figures 8 and 9 present the AFM topographies and accompanying line profiles of the hybrid films, showing the effects of post-thermal treatment on film roughness. Table II summarizes the mean roughness (Ra), root mean square roughness (Rrms), and peak and valley distance (P-V) values of samples with and without post-thermal treatment. The Rrms of the hybrid films decreased from 4.6 to 4.5 nm with heating for 80 h at 90°C, as compared with that of the sample without post-thermal treatment Similar trends could also be seen for mean roughness. This seemed to indicate that post-thermal treatment could not only accumulate TiO_2 particles on each other but also could fill up some of the depressions between particles.

Above all, the surface roughness parameters of the hybrid films, Ra, Rrms, and P-V, were 1.3–2.3, 4.5–4.6, and 9.7–19.4 nm, respectively, indicating the hybrid films had slippery and flat surfaces. This suggests

TABLE II
Roughness of TiO2/Polyacrylate Hybrid Films

Samples	Ra (nm)	Rrms (nm)	P-V (nm)
A[a]	1.3–2.3	4.5	9.7–19.4
B[b]	1.5–2.3	4.6	10.6–18.9

[a] TTB = 30 wt %, 90°C for 80 h, photocuring 6 min.
[b] TTB = 30 wt %, no postheat treatment, photocuring 6 min.

their potential applications in areas such as optic lenses, semiconductor mask films, and wear-resistant materials.

Refractive index

High-refractive-index optical thin film is one type of important optical material. However, the application of organic polymers for high-refractive optical materials is limited because of their low refractive index.[26] Recently, inorganic materials, especially TiO_2, have been used to fabricate high-refractive = index organic–inorganic hybrid materials.

In the present work, the relationship between TTB content and refractive index of the film is shown in Figure 10. It can be seen that the refractive index of the TiO_2 hybrid films increased rapidly at 5 wt % TTB, as compared with that of pure polyacrylate film, and then changed slowly with higher TTB content, indicating that the refractive index of the TiO_2 hybrid films was not proportional to the TTB content.

As demonstrated in the FTIR data (not shown here), a stiff oxide network was formed with the rising TTB concentration; therefore, the contact probability of TiOH groups presenting at the TiO_2 surface decreased, which in turn hindered the completion of the condensation process and further oxide network development and made the refractive index of the films increase slightly with rising TTB concentrations.

In addition, some changes in the refractive index of the TiO_2 hybrid films were induced by irradiation and post-thermal treatment. These changes are shown in Table III.

As expected, post-thermal treatment could increase the hybrid film refractive index—the higher the post-heat temperature, the higher the refractive index of the hybrid films—which could be a result of the densification of the hybrid films during post-thermal treatment. Above all, it appears that the post-thermal temperature can upgrade the refractive index of the hybrid films more dramatically than can post-thermal treatment time.

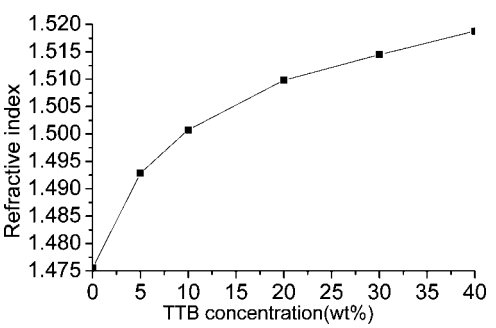

Figure 10 Refractive index of hybrid film as a function of TTB concentration (thermal treatment: 90°C for 80 h).

TABLE III
Refractive Index as Function of Thermal Treatment Temperature and Photocuring Time

	No heat treatment	90°C/ 2 h	90°C/ 56 h	150°C/ 2 h	200°C/ 1 h
Refractive index	1.5047	1.5129	1.5145	1.5188	1.5192

Photocuring time, 6 min; TTB content, 30 wt %.

CONCLUSIONS

Transparent, UV-curable acrylic resin/titania organic–inorganic hybrid films with an improved refractive index and UV-shielding properties were prepared by the sol–gel method in Span85/Tweeen 80 reverse micelles with subsequent *in situ* photopolymerization. UV–vis spectra and atomic force microscopy indicated the presence of a hybrid composite with nanoscale dimensions. During post-thermal treatment, there was an obvious increase in the titania content of the hybrid films at higher temperatures and higher TTB concentrations, whereas there was only a slight increase with longer treatment times. On increasing the inorganic content, the refractive index and UV-shielding properties of the acrylic polymer were greatly improved.

The authors gratefully acknowledge fruitful discussion with Professor Zhang Yong of Chengdu University of Technology on the preparation of nanosized TiO_2. They are also grateful to Ye Yuan and Wen-Qiong He of Chengdu University of Technology for extending all possible facilities.

References

1. Sreekumari, P. N.; Radhakrishnan, T.; Revaprasadu, N.; Kolawole, G. A.; Luyt, A. S.; Djoković, V. Appl Phys A 2005, 81, 835.
2. Smirnova, T.; Sakhno, O.; Bezrodnyj, V. J. Appl Phys B 2005, 80, 947.
3. Izaak, T. I.; Babkina, O. V.; Mokrousov, G. M. Tech Phys 2005, 50, 669.
4. Bhimaraj, P. B.; David, L. A.; Gregory, W.; Toney, C. G.; Siegel, R. W.; Schadler, L. S. Wear 2005, 258, 1437.
5. Nad, S.; Sharma, P.; Roy, I.; Maitra, A. J Colloid Interface Sci 2003, 264, 89.
6. Yoshida, M.; Prasad, P. N. Chem Mater 1996, 8(1), 235.
7. Hu, Q.; Marand, E. Polymer 1999, 40, 4833.
8. Wang, B.; Wilkes, G. L.; Hedrick, J. C.; Liptak, S. C.; McGrath, J. E. Macromolecules 1991, 24, 3449.
9. Lee, L. H.; Chen, W. C. Chem Mater 2001, 13, 1137.
10. Blanchard, J.; Doeuff, S. B.; Maquet, J.; Sanchez, C. New J Chem 1995, 19, 929.
11. Sanchez, C.; Livage, J.; Henry, M.; Babonneau, F. J Non-Cryst Solids 1988, 100, 65.
12. Durand, S. P.; Rouviere, J.; Guizard, C. Coll Surf 1995, 98, 251.
13. Ginzberg, B.; Bilmes, S. A. Progr Colloid Polym Sci 1996, 102, 51.

14. Francois, N.; Ginzberg, B.; Bilmes, S. A. J Sol-Gel Sci Technol 1998, 13, 341.
15. Schubert, U.; Lorenz, N. A. Chem Mater 1995, 7, 2010.
16. Schubert, U.; Arpac, E.; Glaubitt, W. A.; Helmerich, A.; Chauet, C. Chem Mater 1992, 4, 291.
17. Livage, J. Act Chem 1997, 10, 4.
18. Kormann, C.; Bahnemann, D. W.; Hoffmann, M. R. J Phys Chem 1988, 92, 5196.
19. Kandori, K.; Kon-no, K.; Kitahara, A. J Colloid Interface Sci 1988, 122, 78.
20. Madhusudan, R. K.; Gopal, R. C. V.; Manorama, S. V. J Solid State Chem 2001, 158, 180.
21. Kyprianidou, L. T.; Caseri, W.; Suter, U. W. J Phys Chem 1994, 98, 8992.
22. Chang, C. C.; Chen, W. C. J Polym Sci, Part A: Polym Chem 2001, 39, 3419.
23. Chen, W.-C.; Lee, S.-J.; Lee, L.-H.; Lin, J.-L. J Mater Chem 1999, 9, 2999.
24. Chrysicopoulou, P.; Davazogou, D.; Traplis, C. Thin Solid Films 1998, 323, 188.
25. Tang, H.; Prasad, K.; Sanjinès, P.; Schmid, P. E.; Lévy, F. J Appl Phys 1994, 75, 2042.
26. Papadimitrakopoulos, F.; Wisniecki, P.; Bhagwagar, C. E. Chem Mater 1997, 9, 2928.